arXiv:astro-ph/9807180v2 27 Aug 1998

Distribution of Spectral Characteristics and the Cosmological Evolution of GRBs.

Nicole M. Lloyd and Vahé Petrosian
Center for Space Sciences and Astrophysics, Stanford University,Stanford, CA 94305-4060

ABSTRACT

We investigate the cosmological evolution of GRBs, using the total gamma-ray fluence as a measure of the burst strength. This involves an understanding of the distributions of the spectral parameters of GRBs as well as the total fluence distribution - both of which are subject to detector selection effects. We present new non-parametric statistical techniques to account for these effects, and use these methods to estimate the true distribution of the peak of the νF_ν spectrum - E_p - from the raw distribution. The distributions are obtained from four channel data and therefore are rough estimates; hence, we emphasize the methods and present qualitative results. Given its spectral parameters, we then calculate the total fluence for each burst, and compute its cumulative and differential distributions. We use these distributions to estimate the cosmological rate evolution of GRBs, for three cosmological models. Our two main conclusions are the following: 1) Given our estimates of the spectral parameters, we find that there may exist a significant number of high E_p bursts that are not detected by BATSE, 2) We find a GRB co-moving rate density quite different from that of other extragalactic objects; in particular, it is different from the recently determined star formation rate.

Subject headings: gamma rays: bursts – methods: statistical – cosmology: observations – miscellaneous.

1. Introduction

Identification of several gamma-ray bursts (hereafter GRBs) with X-ray, optical and radio afterglows, as well as measurements of the redshifts of GRB 970508, GRB 981214, and GRB 980703 are beginning to define the GRB paradigm. However, this information is not sufficient for detailed cosmological studies of their distribution and evolution. Until more information on the distances to GRBs are revealed, we must continue to rely on standard statistical studies (such as obtaining number count distributions of fluence or flux) to gain further insight on the nature of these events.

However, information on the spatial distribution - although necessary - will not be sufficient for solving the puzzle of GRBs. In particular, we need spectral information to understand the

energy release and radiation processes at the burst. This paper deals with the determination of the spatial and spectral properties of GRBs.

The information on the spatial distribution comes primarily from the investigation of source counts or the log$N$-log$S$ relation. Assuming a luminosity function (LF) and a cosmological model, one can convert such counts to spatial (or redshift) distributions (Weinberg, 1972). The likelihood of the assumed luminosity function determines our confidence in the redshift distribution or cosmological evolution of these sources. The usual practice is to use the peak flux $f_p(\nu)$ as a measure of the burst strength. This flux is related to the peak luminosity $L_p(\nu)$ via $L_p(\nu) = f_p(\nu)\Omega d_L^2 K(z)$, where $d_L(z)$ is the luminosity distance, $K(z)$ is the so-called K-correction due to redshift of the spectrum, and Ω is the solid angle into which the radiation is beamed ($\Omega = 4\pi$ for isotropic emission). However, we have no knowledge of the burst peak luminosity function - say $\Psi(L_p(\nu))$ - and it is unclear what assumptions can be made about this function. For example, in a fireball model, both the duration and the peak luminosities are expected to depend on the details of the fireball (e.g. the bulk Lorentz factor and amount of baryon loading), so that their distributions will be broad and perhaps comparable to the observed range of the peak fluxes. As a result, the luminosity function cannot be readily de-convolved from the spatial distribution, and we cannot get an accurate measure of the burst evolution or spatial distribution from the log$N$-log$S$ diagram.

On the other hand, in a neutron star (or black hole) merger model, the total energy released - represented by the gravitational potential energy of the merging process - is expected to be well defined and have a narrow distribution; this is also most likely true for the "hypernova" model. Hence, we would like to determine what radiative signature is a representative measure of this energy and the strength of the GRB.

As the name "gamma ray burst" implies, the peak gamma-ray flux f_p (or luminsity L_p) of a GRB far exceeds the peak fluxes at other energies. However, until recently, we did not know at what frequency the total radiated energy peaked. The recent X-ray, optical and radio observations of the afterglows - in particular the fact that these fluxes decline more rapidly than $1/t$ (see e.g. Murakami et al., 1997, Galama et al., 1997) indicate that the energy **fluence** in the gamma-ray range is also higher than in any other band. For isotropic emission or a beaming angle independent of wavelength, this implies that the total gamma-ray radiated energy, $\mathcal{E}_{tot}$, is the best measure of the total released energy. Therefore, it is plausible that the distribution of the gamma-ray radiated energy is narrow, so that the total gamma-ray fluence $F_{tot} = \mathcal{E}_{tot}(1+z)/(\Omega d_L^2)$ provides the best indication of the strength of the burst for the log$N$-log$S$ analysis and other investigations (assuming Ω has a narrow distribution). In particular, it is a better measure than the observed fluence F_{obs}, which represents the fluence in some narrow energy range (i.e. the energy range in which the detector triggers).

Note that the relation between the monochromatic flux (or fluence) and the corresponding luminosities require a knowledge of the so called K-correction due to redshift of the spectrum.

This complication is not present in the relation between the total radiated energy and the total gamma ray fluence. It is also important to note that F_{tot} depends on the spectral properties of the burst. Hence, if we want to simplify matters by dealing with the total fluence, we need to understand the spectral distribution $F(\nu)$ of the GRBs.

The primary goal of this paper is to demonstrate how we can obtain information on the cosmological evolution of GRBs, using the observed distribution of F_{tot}. However, for an accurate determination of the distribution of F_{tot}, we need to determine the spectral parameters of each burst. It is common to use the following four parameters (say, in a Band spectrum (1993)) to characterize a burst's spectrum: the photon energy at the peak of the νF_ν spectrum, E_p, the low energy spectral index, α, the high energy spectral index, β, and a normalization A. The best source of data for the purpose of determining these parameters and F_{tot} is the BATSE instrument on board the Compton Gamma-Ray Observatory (CGRO). However, because the BATSE trigger criterion is based on photon counts between 50 - 300 keV (for the 3B catalog), the selection biases or thresholds on F_{tot} as well as the spectral parameters can be quite complicated. In §2 we show how the trigger criterion used by BATSE can be used to obtain the selection bias on any measured quantity - in particular, F_{tot} and E_p - and describe new methods to account for the resultant complicated data truncation. In §3, we present our results on the determination of the spectral parameters. The distribution of E_p is given in §4, and in §5 we derive the distribution of F_{tot}, give a scenario for cosmological evolutions of the GRBs, and discuss its relation to the new observations of afterglows and evolution of other cosmological sources. A brief summary is presented in §6.

2. Description of Data and The Basic Problem

2.1. The Data

BATSE has produced a large catalog of GRBs with a wealth of information on their temporal and spectral characteristics. This detector has been designed to optimally detect GRBs and has been very successful in achieving this goal. Nevertheless, like all detectors, it has intrinsic limitations and may miss certain types of bursts or provide only limited information on others. BATSE is a triggered instrument; it will record data on a burst if the detector counts in a time interval Δt and energy range ΔE exceed some threshold value $C_{min}(\Delta t)$ determined by the background fluctuations. BATSE uses three trigger time intervals $\Delta t = 1024, 256,$ and 64 ms with four energy channels $\Delta E = 25-50, 50-100, 100-300,$ and > 300 keV. For most of the data, triggering is based on counts in channels 2 and 3; recently, however, other channel combinations have been tried. Here we will use the 4 channel LAD fluence values published in the BATSE 3B catalog (Meegan et al., 1995), which utilizes the former trigger scheme, so that the observed fluence $F_{obs} \equiv \int_{50keV}^{300keV} F(\nu)d\nu$. However, the formalism described below is applicable to the latter data as well. Note that we analyze bursts with C_{max}/C_{min} on 1024ms timescale. Because of the lack of resolution of the four channel data, here we will emphasize the method of our calculations

rather than give concrete quantitative results. Future work will involve calculations made from 16 channel CONT data.

2.2. Data Truncation

The BATSE detector trigger conditions lead to several limitations on the data. The most obvious is that only bursts with peak counts $C_{max} > C_{min}$ are detected. Determination of the average $V/V_{max} = (C_{min}/C_{max})^{3/2}$, and its distribution were one of the primary objectives of BATSE using this trigger configuration (Meegan et al., 1992). Another limitation arises from the finite durations Δt of the triggering criteria. As pointed out by Petrosian and Lee (1994, see also Lee and Petrosian, 1996), this reduces the detector efficiency of short duration bursts (duration $T < \Delta t$) in the sense that there is a relative bias against detection of weaker bursts with shorter duration. Similarly, as pointed out by Piran and Narayan (1996), the finite range ΔE of the detector energy channels provides another limitation (see also Cohen, Piran, and Narayan, 1998). In this case, the detector efficiency is highest for bursts with most of their photons in the range ΔE, and decreases for bursts with more of their flux outside this range.

It turns out that we can account for these limitations by utilizing the BATSE trigger condition: Let us consider a burst characteristic, say X, whose value is measured by BATSE. For each burst, then, we know X, C_{max}, and C_{min}. Now, in the spirit of the V/V_{max} test, one can ask what is the possible range of values of X that this burst can have and still trigger the instrument. In general, X can have an upper limit u, a lower limit l, or both limits; $X \in T = [l, u]$. This question was first posed by Petrosian and Lee (1996) in connection with the determination of the detection threshold or efficiency of the observed energy fluence F_{obs}; in this case, the fluence has only a lower limit $F_{obs,lim}$. It was shown that this threshold (or for that matter, the threshold on any other measure of burst strength which is proportional to the photon counts) is obtained from the simple relation

$$F_{obs}/F_{obs,lim} = C_{max}/C_{min}, \tag{1}$$

provided the burst's spectrum does not change drastically throughout its duration. A similiar relation holds for the total fluence F_{tot} as we describe in §5.

For other bursts characteristics, this may not be the case. For example, we have shown (Lloyd and Petrosian 1998) that the spectral parameter E_p has both an upper and lower limit. The values of $E_{p,max}$ and $E_{p,min}$ are not related to C_{max}/C_{min} and E_p in a simple form as above, and thus we require a more complex procedure to determine their values. We will describe this in §3. Given the thresholds, we can then use non-parametric statistical techniques to obtain an estimate the parent distribution of the relevant observable from the observed distribution.

2.3. Dealing with Data Truncation

Correcting for data truncation in the one-sided case was discussed in detail by Efron and Petrosian (1992). This method has been used to determine the correlation between parameters in a bivariate (or multivariate) setting, and to obtain univariate distributions of several GRB characteristics (see, e.g., Lee and Petrosian, 1996). The basic idea is that one can use information from the untruncated region of a distribution to estimate how much data is missed due to the truncation. For a description of the basic process, see also Petrosian (1992 or 1993).

Dealing with data which has both upper and lower limits is more complex and requires a generalization of the above technique. Recently, Efron and Petrosian (1998) have developed a method to deal with this kind of data truncation. We briefly review this method here.

Consider data points (x_i, y_i) (in our case (E_p, F_{obs})), where x_i has lower and upper limits l_i and u_i, respectively; $x_i \in T_i = [l_i, u_i]$. Let us also assume that x_i and y_i are uncorrelated. Let $g(x)$ be the true distribution of x, which would be observed if there were no truncations. However, because x_i is limited to T_i, we observe the conditional distribution $g(x_i|T_i) = g(x_i)/G(T_i)$, where $G(T_i) = [\sum_j g(x_j) : x_j \in T_i]$ is the probabilitly that x exists in T_i. We normalize $g(x_i)$ such that $\sum_{i=1}^{N} g_i = 1$, and define the vectors

$$g_i = g(x_i) \quad \text{and} \quad G_i = G(T_i) \tag{2}$$

and the matrix

$$J_{ij} = \begin{cases} 1, & x_j \in T_i, \\ 0, & x_j \notin T_i. \end{cases} \tag{3}$$

Furthermore, by definition, one can show that $G_i = J_{ij} g_j$ (where we have used the convention that repeated indices are summed over). The goal is to estimate $g(x)$ from l_i, u_i, and x_i assuming all N cases are independently distributed. It can be shown that maximizing the likelihood (see Maloney et al., 1998) of the observed data set gives

$$1/g_i = J_{ji} * (1/G_j) + \text{const}, \tag{4}$$

where J_{ji} is the transpose of J_{ij}. The procedure amounts to solving this equation iteratively, under the normalization condition and definition of G_j and J_{ij} given above. Convergence is reached when *const* in the above equation goes to zero. This method can be used to determine univariate cumulative (G) and differential (g) distributions. As described in Efron and Petrosian (1998), it can also be used to determine correlations between relevant variables (e.g. fluence and E_p or peak flux and E_p).

We will use the methods described above to correct for data truncations and produce bias free distributions of the peak energy E_p and the total fluence F_{tot}; we will then directly use the latter distribution to investigate the cosmological evolution of GRBs.

3. Spectral Characteristics

The spectral properties of GRBs provide the most direct information about the physical processes associated with the event. In particular, the distribution of the spectral parameters and the correlation between these and other GRB characteristics can shed significant light on the radiation mechanisms and energy production of the burst.

Therefore, our first task is to determine the spectral parameters of each burst. We characterize the spectral forms of the bursts by four parameters - α and β (the photon power law index at low and high energies respectively), E_o (a break energy related to the peak of the νF_ν spectrum) and A (a normalization in units of $ergs/cm^2$). We choose two functional forms to represent the **energy** fluence spectra - a Band spectrum, and a generic double power-law spectrum with a smooth transition between the low energy and high energy power law behavior:

$$F(E) = \begin{cases} (A/E_o)(E/E_o)^{\alpha+1}\exp[(\beta-\alpha)(E/E_o-1)], & E < E_o \\ (A/E_o)(E/E_o)^{\beta+1}, & E > E_o \end{cases} \tag{5}$$

$$F(E) = \frac{(A/E_o)(E/E_o))^{\alpha+1}}{1+(E/E_o)^{\alpha-\beta}} \tag{6}$$

We are interested in bursts whose νF_ν spectra have a maximum, so that we may correctly speak of E_p as the "peak of νF_ν ". To define E_p (as well as to keep the burst's total fluence F_{tot} finite), we require α to be greater than -2 and β to be less than -2 (which also implies $\alpha > \beta$). As we discuss below, this does not impose any large bias in our sample. Then, with these constraints, we can define E_p for each spectrum above: $E_p = E_o(\frac{\alpha+2}{\alpha-\beta})$ and $E_p = E_o(\frac{-(\beta+2)}{\alpha+2})^{\frac{1}{\beta-\alpha}}$ for (5) and (6), respectively.

From four channel data, we can determine the four spectral parameters with no degrees of freedom. However, this introduces strong interplay between E_p and β or α. We avoid this by selecting β from an assumed gaussian distribution with a mean of ≈ -3, and a standard deviation of 1 (and of course the constraint $\beta < -2$). This allows for one degree of freedom. In fact, we have performed this analysis using several distributions for β (i.e. a uniform distribution, or a gaussian with a different mean and standard deviation), and have found similiar qualitative results. However, we should note that steeper, more negative β's will naturally produce higher E_p's, to accommodate the fluence in high energy channels (3 and 4). We find the rest of the parameters by minimizing χ^2 via a downhill simplex routine (e.g. see Press et al., 1992). For the Band spectrum, we find acceptable fits for 291 bursts, while 268 give acceptable fits for the second spectrum listed above, out of a total of 518 bursts. Figures 1(a) and 1(b) show the raw distributions of the spectral parameters obtained with this method for the two spectral forms in equation 5 and 6, respectively.

It turns out that the distribution of the parameters for bursts with unacceptably high χ^2 is not very different from those with acceptable χ^2. We have tested to see if the reason for many high χ^2 bursts came from the constraints on α and β mentioned above. Relaxing these restrictions, we found that only $\sim 1\%$ of bursts that gave acceptable fits had an $\alpha < -2$, $\beta > -2$, or $\alpha > \beta$. We

therefore assume that the bursts with good fits are representative of the total sample. However, because the lack of energy resolution of the four channel data, we would like to emphasize that our fits are rough estimates of the actual spectral parameters, so that the following analysis exhibits our method rather than presenting a final quantitative result. As mentioned previously, in future work we will use fits from 16 channel CONT data, which will provide a more accurate determination of these parameters.

Several studies have obtained the spectral parameters for the brightest GRBs (e.g., Band et al. 1993) and investigated correlations between these parameters and peak flux, duration and spatial distributions (Mallozzi et al. 1995, Kouvelioutou et al. 1995, Pendleton et al. 1996). However, caution is required in such studies, when dealing with the raw data. The effects of selection biases must be evaluated before obtaining these distributions and correlations. The parent distributions of the spectral parameters could be quite different from the observed distributions shown in the above figures. The differences are caused by the truncations resulting from the triggering procedure, and are a measure of trigger efficiencies for each of the four spectral parameters α, β, E_p, and A or $F_{tot} = A\xi(\alpha, \beta)$. The truncation on A or F_{tot} is described by equation (1): $F_{tot,lim} = F_{tot}(C_{min}/C_{max})$. As mentioned previously and shown in detail in the next section, there are also selection biases against high and low values of E_p. For instance, BATSE is most likely to see bursts with E_p in the energy range in which the detector triggers. Becuase the detector needs some minimum number of counts C_{lim} to trigger, then for each burst one can find an interval $[E_{p_{min}}, E_{p_{max}}]$ to which E_p is confined in order for the burst to have been detected.

Similarly, truncation is present for α and β. For example, if a burst with given E_p and A had a value of α which was postitive and large or had a value of β which was negative and large, - i.e. if the νF_ν spectrum had a steep rise or fall - then the observed C_{max} could fall below the threshold C_{min} and render the burst undetectable. Using the methods described in §2 and below, we can correct the raw distribution of all four parameters and determine their correlations with other GRB characteristics. However, the effect of the truncation on α and β is more complicated and not as pronounced as that of E_p and F_{tot}. We will deal with the former in future publications. Here, we limit our discussion to obtaining the true distributions of E_p and F_{tot}. We will present the results from the Band spectrum fits to the bursts only; the smooth double power-law spectrum in equation (6) gives qualitatively similiar results for all of the following analysis.

4. Distribution of E_p

For each burst we have the values of α, β, A, E_p, and the observed fluence $F_{obs} = \int_{E_1}^{E_2} F_{\alpha,\beta,A}(E, E_p)dE$, with $E_1 = 50keV$ and $E_2 = 300keV$. From equation 1, we can calculate the fluence threshold $F_{obs,lim}$. Using this limit, we can determine the possible range of values E_p can take on, and still trigger the BATSE instrument. It is clear that the limiting

value $E_{p,lim}$ must satisfy the equation

$$F_{obs,lim} = \int_{E_1}^{E_2} F_{\alpha,\beta,A}(E, E_{p,lim}) dE. \quad (7)$$

For the spectral forms and parameter ranges discussed in the previous section, the right hand side of equation (7) increases monotonically with $E_{p,lim}$, reaches a maximum for $E_{p,lim}$ within the limits of the integration, and then decreases monotonically. Consequently, there will be two values of $E_{p,lim}$ that satisfy this equation. To find these two solutions, we start with the value of E_p determined by the simplex routine (for which the right side is equal to F_{obs}), and increase it (while keeping α, β, and A equal to their determined values) until equation (7) is satisfied - that is, until the observed fluence is brought below the threshold. This value is the upper limit to E_p, $E_{p,max}$. We then decrease E_p until this equation is again satisfied. This gives the lower limit $E_{p,min}$. In essence, the procedure amounts to redshifting/blueshifting the burst until it is undetectable by BATSE. Figure 2 shows E_p vs. $E_{p,max}$ and $E_{p,min}$ for the Band spectrum. Notice the truncation is much more prominent on the upper than the lower end; hence, we expect to see a more significant correction to the high end of the E_p distribution.

Using the method described in §2.3 for doubly truncated data, we corrected the observed distribution given that the observations can detect only bursts with E_p limited to the interval $[E_{p_{min}}, E_{p_{max}}]$. Figure 3 shows the raw and corrected differential distribution of E_p for the Band spectrum. The raw and corrected distributions are normalized such that they are equal at low values of E_p (where the data truncation is inconsequential). This normalization visually emphasizes the differences of the distributions at high E_p. The figures suggest that a large number of high E_p bursts are missed by the triggering procedure.

In order to determine the significance of the difference between the raw and corrected distributions, we carry out the following two checks: First, we perform a K-S test on the cumulative distributions of E_p, and a χ^2 test on their differential distributions for both the Band spectrum and the smooth double power law. For the χ^2 test, we divide the distributions into two bins, with equal numbers of observed bursts per bin. As shown in the table below, in both cases the tests indicate the probability that the observed and corrected E_p distributions are the same is extremely small.

Test	Spectrum	Probability the distributions same
K-S	Band	1.8×10^{-6}
χ^2	Band	3.0×10^{-7}
K-S	Double Power Law	4.4×10^{-5}
χ^2	Double Power Law	2.4×10^{-5}

Second, we have carried out simulations to determine the accuracy of the method described in §2.3; Appendix A contains these results. We begin with a parent distribution of E_p's, simulate an

observational truncation (defined by the limiting fluence of the burst; see §4). From this we obtain our observed distribution of E_p's. We then apply the above technique to correct for the truncation, and retrieve our parent distribution to very high accuracy, demonstrating the robustness of the method (see Appendix A for more details).

Our results are in qualitative agreement with the observational data from the Solar Maximum Mission (SMM) presented by Harris and Share (1998a, 1998b); SMM is sensitive to higher energies than BATSE, so that it suffers the bias against detection of bursts with hard spectra to a much lesser degree. The results presented in Harris and Share (1998b) agree qualitatively with our corrected E_p distribution. We perform a similiar χ^2 as above, comparing the E_p distribution from SMM with both the uncorrected and corrected BATSE E_p distributions presented in Figure 3. In this case, we divide the data into two bins below and above 550 keV. We find the probability that the E_p distribution from SMM data is the same as the raw BATSE E_p distribution to be 1.3×10^{-6}. On the other hand, we find a 90% probability that the E_p distribution from the SMM data is the same as the corrected BATSE E_p distribution. Note that the statistical method we use can correct the E_p distribution only for the values of E_p observed by BATSE. Therefore, we cannot determine the distribution above ~ 1 MeV (where the raw BATSE distribution ends). Similarly, because we have no observed E_p's below ~ 20 keV, we cannot confirm Strohmeyer et al. (1998) reporting a significant number of low E_p bursts (< 20 keV) observed by GINGA, but not observed by BATSE.

A bias against detection of high E_p bursts has significant implications on correlations of E_p with other measures of burst strength like peak flux, F_{obs}, or F_{tot}. The detector is most likely to miss the high E_p bursts with low strength, so that a simple correlation analysis between raw values of E_p and burst strength without the consideration of the data truncation can lead to erroneous correlations. Examples of studies which may be affected by such a bias include the correlation studies of Nemiroff et al. (1994) and Mallozzi et al. (1995). This will also have an important effect on determining whether or not the correlations are intrinsic or due to cosmological redshift (Brainerd, 1997). The above results indicate that a more thorough analysis of the correlations is required before conclusions can be reached on the redshifts or intrinsic effects. We will address this question in a future publication, when we have more accurate estimates of the spectral parameters.

5. Distribution of the Total Gamma Ray Fluence

As discussed in the introduction, an important way to learn about the spatial distribution of GRBs is to study the distribution of some standard candle variable of the event. We also conjecture the total radiated energy $\mathcal{E}_{tot}$ in the gamma-ray range may be the best candidate for such a standard candle variable, and that the total fluence F_{tot} of the GRB may provide the best measure of distance. Consequently, we study the distribution of the bursts' total fluence; if the

burst radiates isotropically, the total fluence is related to the total radiated energy $\mathcal{E}_{tot}$ as:

$$F_{tot} = \frac{\mathcal{E}_{tot}}{4\pi d_L^2}(1+z), \tag{8}$$

where d_L, the luminosity distance, depends on redshift and the cosmological model (Weinberg, 1972).

Again, because the detector is sensitive only over a finite energy range, BATSE does not necessarily obtain all photons from the burst. Hence, the detector measures only a portion of the burst's total fluence. However, the total fluence of a GRB can be obtained from the spectral fits to the observed fluence simply by integrating over the spectrum of that burst: $F_{tot} = \int_{E_{min}}^{\infty} F_{\alpha,\beta,A}(E, E_p)dE.$, where E_{min} denotes the beginning of the gamma ray energy range (as an estimate, we use $E_{min} = 25$ keV). This fluence will have an observational lower limit in the same way that the fluence from $50 - 300$ keV has, and its threshold is given by the generalization of equation (1): $F_{tot,lim} = \frac{C_{min}}{C_{max}} F_{tot}$. Following the steps described in Petrosian and Lee (1996), we first test for any correlation between F_{tot} and $F_{tot,lim}$ and parametrically remove this correlation. We then use the method described in Efron and Petrosian (1994) for one sided truncated data (this is equivalent to the method of §2.2, taking the upper limit u to ∞), and obtain the cumulative and differential distributions for the total fluence.

Figures 4(a) and 4(b) show the cumulative and differential distributions of the total and observed fluence for our sample. Marked on each curve are GRB 970508 (circle), GRB 971214 (cross), and GRB 980703 (triangle). Note that we do not find a good spectral fit for GRB 980703; hence, we obtain a lower limit to its total fluence simply by summing up the published fluence values for the four channels of the LAD detector. Following the tradition of radio astronomers (see Lee and Petrosian, 1996), we divide out the $-3/2$ power law dependence of the number on the total fluence. In this way, deviation from the horizontal line suggests deviation from a homogeneous, isotropic, static, Euclidean distribution. In these figures, we have included all 518 bursts available - including those whose spectral fits gave high values of χ^2 - so as not to underestimate any part of these distributions. We have also applied the same procedure to the subsample of bursts with acceptable values of χ^2 and find that the distributions are similiar to those of the complete sample within about 30 %. Note that the fluence distributions in Figures 4(a) and 4(b) are unlike the counts of other well known extragalactic sources such as galaxies, radio sources and AGNs or quasars. The transition from 3/2 power law is too abrupt and the slope beyond this transition is nearly constant. Clearly, some extraordinary evolutionary processes are at work. We explore this in more detail in the next section.

5.1. Rate Evolution

There have been several detailed analyses of the log$N$-log$S$ distribution for the peak fluxes of GRBs with inconclusive results. This is primarily because any observed distribution can be fitted

to an arbitrary luminosity function and evolution even if one assumes a cosmological model (see e.g. Rutledge et al. 1995, Reichert and Mészáros, 1997, Mészáros and Mészáros, 1995, Hakkila et al., 1996). Additional uncertainty associated with these results comes from neglect of the time bias, spectral bias, and uncertainty in the value of the K-correction. These source of error are absent when dealing with the total fluence, which requires no correction for time bias (Lee and Petrosian, 1996), includes the spectral bias (described above), and requires no K-correction. Thus, the relation between the total fluence counts and either the cosmological models or the luminosity function and its evolution is more straight forward. Here we concentrate on the rate evolution of GRBs.

To obtain some indication of possible evolution, we assume several representative values for the total radiated energy $\mathcal{E}_{tot}$ and derive the comoving rate density from the observed differential counts of the fluences as

$$\rho(z) = (1+z)n(F_{tot})(dV/dz)^{-1}(dF_{tot}/dz) \tag{9}$$

where $n(F_{tot})$ is the differential distribution of the total fluence. Note that in all of our calculations, we have assumed $H_o = 60\text{km s}^{-1}\text{Mpc}^{-1}$

Figures 5(a), 5(b) and 5(c) show $\rho(z)$ for three representative cosmological models. In order to span the range of possible evolutions, we choose three extreme models: a flat matter dominated model ($\Omega_m = 1$, $\Omega_\Lambda = 0$), a curvature dominated model ($\Omega_m = 0.2$, $\Omega_\Lambda = 0$), and a flat vacuum energy dominated model ($\Omega_m = 0$, $\Omega_\Lambda = 1$). Here, Ω_m is the density parameter (equal to the ratio of matter density to the critical density), and $\Omega_\Lambda = \Lambda c^2/3H_o^2$ (where Λ is the cosmological constant). Within each figure, $\rho(z)$ is plotted for four standard candle energies: $\mathcal{E}_{tot} = 10^{51}$, 10^{52}, 10^{53}, 10^{54} ergs. Superposed on each figure is the star formation rate (SFR) from Madau et. al (1997, solid line), this rate delayed by 2×10^9 years (dashed-dot line), as well as the SFR convolved with a distribution of time delays $P(t) \propto t^{-1}$ (dotted curve), which may arise in a neutron star or black hole merger scenario (see e.g. Totani, 1997). Note that the SFR was calculated using an $\Omega_m = 1$, $\Omega_\Lambda = 0$ cosmology (Madau, 1997); however, the shape of this curve as well as the 2 other curves derived from the SFR are fairly insensitive to the cosmological model (see e.g., Totani, 1997).

Also marked on each figure are the rate densities of GRB 970508 (circle), GRB 971214 (cross) and GRB 980703 (triangle), given their measured redshifts, and the energy $\mathcal{E}_{tot}$ required to produce a burst at this redshift (given its total fluence). Table II lists this required energy. Again, because we have only obtained a lower limit to the total fluence of GRB 980703, we only list a lower limit to its required radiated energy.

Burst	Redshift	$F_{tot}\ ergs/cm^2$	Cosmology	Required $\mathcal{E}_{tot}\ ergs$
GRB 970508	0.83	7.0×10^{-6}	$\Omega_m = 1\ \Omega_\Lambda = 0$	1.0×10^{52}
GRB 970508	0.83	7.0×10^{-6}	$\Omega_m = 0.2\ \Omega_\Lambda = 0$	1.4×10^{52}
GRB 970508	0.83	7.0×10^{-6}	$\Omega_m = 0\ \Omega_\Lambda = 1$	2.5×10^{52}
GRB 971214	3.43	1.2×10^{-5}	$\Omega_m = 1\ \Omega_\Lambda = 0$	1.7×10^{53}
GRB 971214	3.43	1.2×10^{-5}	$\Omega_m = 0.2\ \Omega_\Lambda = 0$	4.4×10^{53}
GRB 971214	3.43	1.2×10^{-5}	$\Omega_m = 0\ \Omega_\Lambda = 1$	1.8×10^{54}
GRB 980703	0.97	$> 6.1 \times 10^{-5}$	$\Omega_m = 1\ \Omega_\Lambda = 0$	$> 1.1 \times 10^{53}$
GRB 971214	0.97	$> 6.1 \times 10^{-5}$	$\Omega_m = 0.2\ \Omega_\Lambda = 0$	$> 1,6 \times 10^{53}$
GRB 971214	0.97	$> 6.1 \times 10^{-5}$	$\Omega_m = 0\ \Omega_\Lambda = 1$	$> 3.2 \times 10^{54}$

In all cases, the curve corresponding to $\mathcal{E}_{tot} = 10^{51}$ ergs is ruled out by the observational data. The $\mathcal{E}_{tot} \geq 10^{52}$ ergs curve accommodates GRB 970508, while GRB 971214 and GRB 980703 require $\mathcal{E}_{tot} > 10^{53}$ ergs. In the $\Omega_\Lambda = 1$ case, the required $\mathcal{E}_{tot} > 10^{54}$ ergs for GRB 971214 begins to exceed theoretical limits, which may be evidence against this cosmological model or evidence for strong beaming of the burst radiation. Our results suggest that the total gamma-ray radiated energy is not a standard candle and is spread over at least one decade. We emphasize that these results depend critically on the total fluence, which in turn depends on accurate values for the spectral parameters for these bursts. Higher resolution fits to the data as well as more measurements of the redshifts of bursts will allow us to constrain the curves more definitely.

Finally, note that none of the three curves for $\rho(z)$ follow the star formation rate curve, as one would expect in many GRB models such as the merger or hypernovae models. The density evolution for GRBS in unlike that for AGN's or ordinary galaxies as well. The results agree - at least qualitatively - with those of Totani (1998). However, this is in contradiction with recent claims that the GRB rate follows the star formation rate (Wijers et al., 1998).

6. Summary and Conclusion

The primary aim of this paper has been to investigate the cosmological evolution of GRBs, which involves understanding the distributions of the spectral parameters as well as the total fluence of the burst. Selection effects limit the information we can observe to explore these distributions.

We have presented new non-parametric methods to account for these effects. We have applied these methods first to the distribution of the peak of the νF_ν spectrum, E_p. We find that this spectral characteristic suffers both upper and lower thresholds, although the upper threshold has the dominant effect. We correct the observed distribution for this truncation and present the parent distribution of E_p. This contains a large number of high E_p bursts not evident in the observed distribution, which is in qualitative agreement with the SMM results of Harris and Share

(1998b). This is important for studying correlations between E_p and other burst characteristics, as well as for theoretical considerations concerning GRB models.

Using the spectral fits for each burst, we determine a rough measure of the total gamma-ray fluence and present the GRB source counts based on this measure. We obtain both the differential and cumulative counts of the total and observed fluences.

We convert these distributions to the comoving rate density of GRBs for 3 different cosmological models and 4 different values of the total gamma ray radiated energies. We find that none of the curves follow the star formation rate as predicted by various GRB models. More observations on the redshifts of GRBs as well as high resolution spectral data (to obtain a precise value for the total fluence) are needed to substantiate these results.

As a final note, we summarize some of the caveats in our analysis. First, the spectral parameters are determined based on four channel data and are only rough estimates of the true spectral properties of the burst. In particular, because β is chosen from an assumed distribution, the correction to the E_p distribution could be overemphasized. These spectral parameters also affect the values of the total fluence (since $F_{tot} = \int F_{\alpha,\beta,A}(E, E_p)dE$), which in turn affect the density evolution functions for the bursts. Furthermore, to derive the density curves, we have assumed that the bursts total fluence is a standard candle; although this seems to be the most plausible candidate for a standard candle, the observations of GRB 970508, 971214, and GRB 980703 indicate the contrary. Note, however, that we can use a standard candle upper and lower limit to at least constrain the possible evolution of GRBs. Finally, effects such as beaming were not taken into account in the density evolution analysis. For a burst beamed into a solid angle Ω, the total radiated energy $\mathcal{E}_{tot}$ will decrease by a factor of $\Omega/4\pi$ from the isotropic total radiated energy; hence, the observed dispersion in the total radiated energy (about an order of magnitude or higher) could be due to variation in the degree of beaming. Meanwhile, beaming causes the number of burst occurances over some time interval to increase by a factor of $4\pi/\Omega$. We will address the issue of how beaming can affect the cosmological rate evolution in a future publication.

We would like to acknowledge P. Madau for the star formation rate data used to generate the three SFR curves in 5(a),5(b), and 5(c). We would also like to thank B. Efron for help in implementing the statistical methods discussed in the text. Finally, N.M. Lloyd would like to thank members of the BATSE team for many useful discussions, and their hospitality during her visit to MSFC.

A. Appendix

Here, we describe the results of simulations which exhibit the technique and demonstrate the accuracy of the procudure used for correcting doubly truncated data. For this analysis, we use the Band spectrum displayed in equation 5. We pull E_p from a uniform distribution between 5 and 35 keV. α is also drawn from a uniform distribution ranging between -0.9 and 5.9, as was β

which ranged from -9.0 to -2.1. Finally, our normalization parameter A is taken from a uniform distribution from 12×10^{-9} to 18×10^{-9}ergs/cm^2. Note that we are not trying to simulate the real distribution of any of these parameters - we choose these distributions for the purpose of displaying selection effects and to what degree our method can account for them.

Once we have the spectral parameters, we can calculate the fluence in each of the four BATSE LAD energy channels. The limiting fluence of each burst is chosen from a gaussian distribution with a mean of 6×10^{-11}ergs/cm^2 and a standard deviation of 6×10^{-10}ergs/cm^2 (note again, this is not an attempt to simulate the actual BATSE detector response). We then ask the question: How many of the 1000 simulated bursts have their fluence in channels 2 and 3, greater than the limiting fluence? We find 554 bursts survived this cut - we will call this the observed sample. We then proceed to apply the method described in §2 to our observed sample, to see if we could get back the original distribution of E_p's. Figure 6 shows the the parent sample, the observed sample, and the correction to the observed sample. As evident, the correction accounts for the truncated data, and approximately reproduces the original sample. See §2 for a full description of the technique.

REFERENCES

Band, D., et al. 1993, ApJ, 413, 281

Brainerd, J.J. 1997, ApJ, 487, 96

Cohen, E., Piran, T., Narayan, R. 1998, ApJ, 500, 888

Efron, B. & Petrosian, V. 1992, Ap.J., 399, 345

Efron, B. & Petrosian, V., JASA, in press

Galama, T., et al. 1997, in Gamma Ray Bursts, AIP Conf. Proc. 428, eds. C.A. Meegan, R.D. Preece, T.M. Koshut (New York: AIP) , 478

Hakkila, J., et al. 1996, in Gamma Ray Bursts, AIP Conf. Proc. 307,eds. G.J. Fishman, J.J. Brainerd, K.Hurley (New York: AIP), 387

Harris, M.J. & Share, G.H. 1998a, in Gamma Ray Bursts, AIP Conf. Proc. 428, eds. C.A. Meegan, R.D. Preece, T.M. Koshut (New York: AIP), 314

Harris, M.J. & Share, G.H. 1998b, ApJ, 494, 724

Horack, J.M., Emslie, A.G., Hartmann, D.H. 1995, ApJ, 447, 474

Kouveliotou, C., et al. 1995, in Gamma Ray Bursts, AIP Conf. Proc. 384, eds. C Kouveliotou, M.S. Briggs, G.J. Fishman (New York: AIP), p.42

Kulkarni, S., et al. 1998, Nature 393, 35

Lee, T. & Petrosian, V. 1996, ApJ, 470, 479

Lloyd, N.M & Petrosian, V. 1997, in Gamma Ray Bursts, AIP Conf. Proc. 428, eds. C.A. Meegan, R.D. Preece, T.M. Koshut (New York: AIP) , 67

Madau, P. 1997, astro-ph/9709147

Mallozzi, R.S., et al. 1995, ApJ, 454, 597

Maloney, A. & Petrosian, V. 1998, ApJ, in press

Meegan, C., et al. 1992, Nature, 355, 143

Meegan, C., et al. 1995, ApJS, 106, 65

Mészáros, P. & Mészáros, A. 1995, ApJ, 449, 9

Metzger et al. 1997, Nature, 387, 879

Murakami, T. et al. 1997, in Gamma Ray Bursts, AIP Conf. Proc. 428, eds. C.A. Meegan, R.D. Preece, T.M. Koshut (New York: AIP) , 435

Nemiroff, R.J., et al. 1997, ApJ, 435, L113

Pendleton, G.N., et al. 1996, ApJ, 464, 606

Petrosian, V. 1992, in Statistical Challenges in Modern Astronomy, eds. E.D.Feigelson and G.J. Babu (New York: Springer-Verlag), 173.

Petrosian, V. 1993, ApJ, 402, L33

Petrosian, V. & Lee, T. 1996, ApJ, 467, L29

Piran, T. & Narayan, R. 1995, in Gamma Ray Bursts, AIP Conf. Proc. 384, eds. C Kouveliotou, M.S. Briggs, G.J. Fishman (New York: AIP), 233

Press, W. H., Teukolsky, S. A., Vetterling W. T., and Flannery,B. P. 1992, Numerical Recipes in FORTRAN (Cambridge: Cambridge University Press)

Reichert, D.E. & Mészáros, P. 1997, ApJ, 483, 597

Rutledge, R.E., et al. 1995, MNRAS, 276, 753

Strohmeyer, T.E., et al. 1997, astro-ph/9712332

Totani, T. 1997, ApJ, 486, L71

Totani, T. 1998, astro-ph/9805263

Weinberg, S. 1972, Gravitation and Cosmology: Principles and Applications of the General Theory of Relativity (New York: Wiley)

Wijers, R.A.M., et al. 1998, MNRAS, 294, L13

This preprint was prepared with the AAS LaTeX macros v3.0.

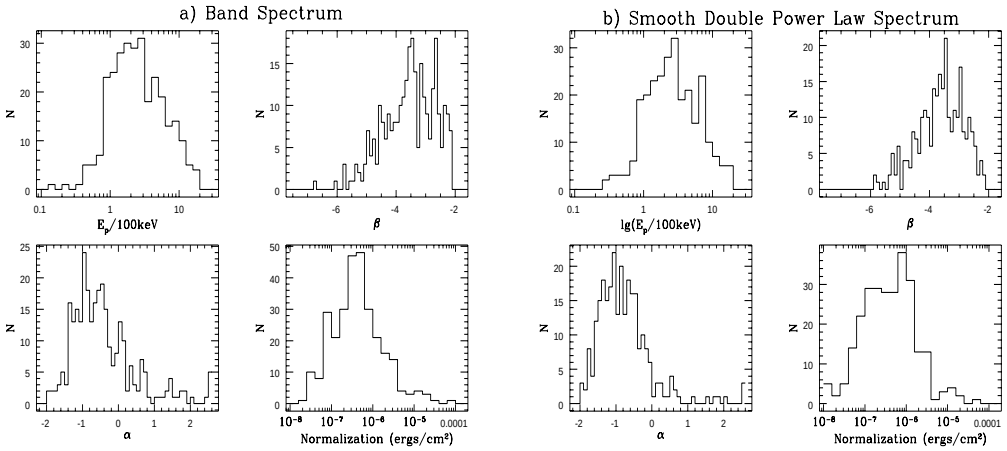

Fig. 1.— The distribution of the spectral parameters determined from a) the Band spectrum and b) a smooth double power-law spectrum respectively. Note that β is drawn from the same truncated gaussian distribution in both cases, and is not a fitted parameter.

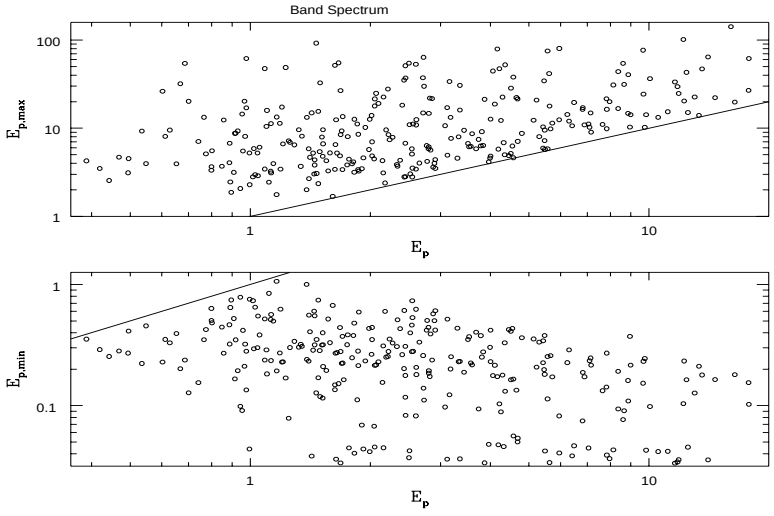

Fig. 2.— The maximum and minimum values of E_p for the Band spectrum. Note that the truncation is more severe from above than below, which indicates that observations may miss a population of GRBs with high E_p.

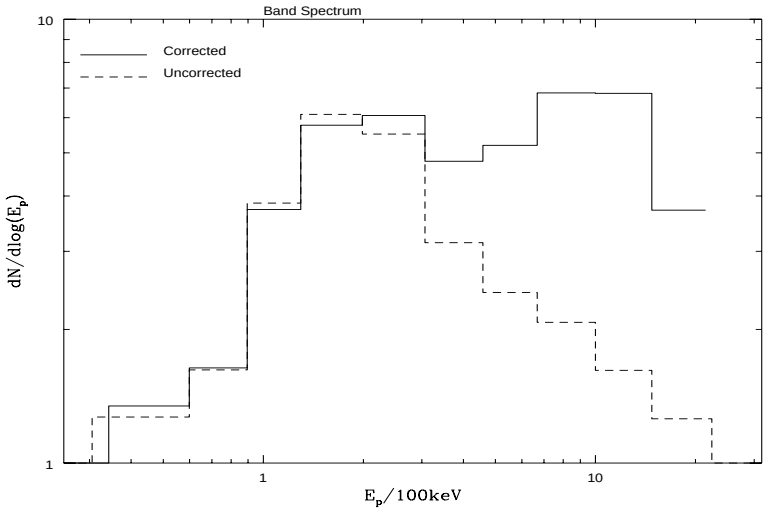

Fig. 3.— The observed and "corrected" distribution of E_p for the Band spectrum. The figure suggests that there is a significant sample of high E_p bursts undetected by BATSE. As mentioned in the text, the methods we used will not produce a correction beyond the raw observed distribution.

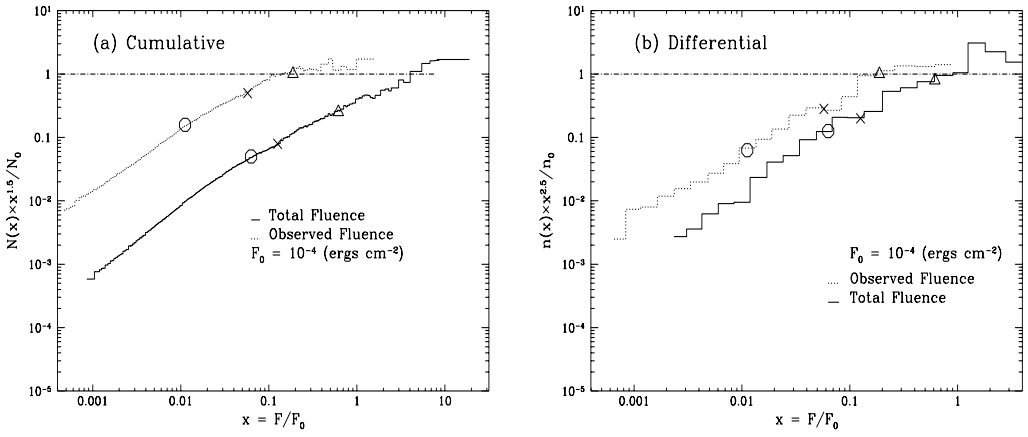

Fig. 4.— The cumulative (a) and differential (b) distribution of both the observed (F_{obs}) and total (F_{tot}) fluences. The circle indicates the observed and total fluences of GRB 970508, the cross marks GRB 971214, and the triangle marks GRB 980703. In each figure, note the similarities between the two distributions; they both display an abrupt break from the HISE dependence (see text), indicating presence of strong evolutionary processes.

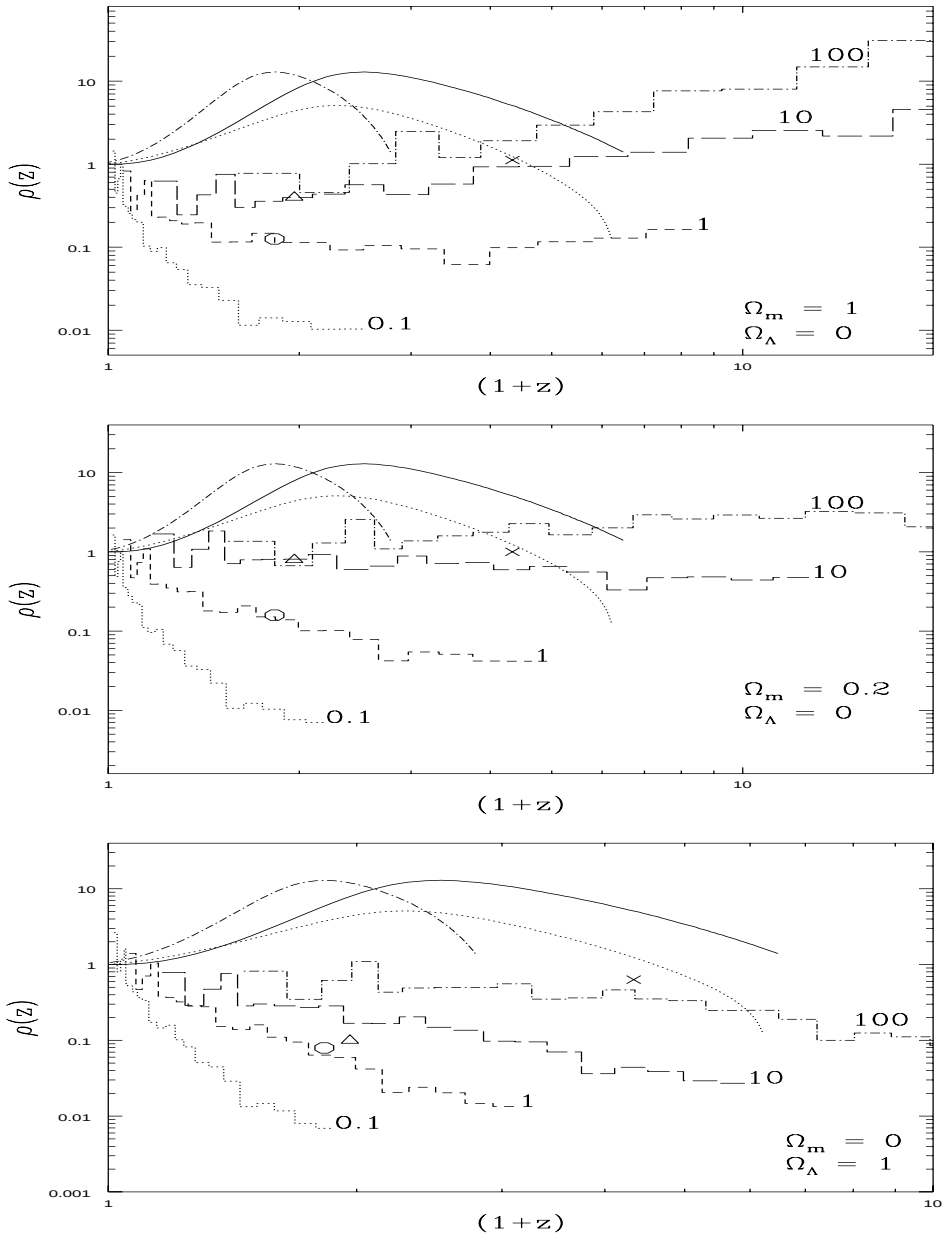

Fig. 5.— The comoving rate density versus redshift z for 3 different cosmological models indicated by the values of Ω_m and Ω_Λ. Within each plot, we show the rate density for 4 different standard candle energies; the numbers 0.1, 1, 10, and 100 mark the total gamma-ray radiated energy in units of 10^{52} ergs. Note that these curves are significantly different from: 1) the star formation rate (SFR) from Madau et al., 1997 (solid line), 2) the star formation rate with a time delay of 2×10^9 yr (dot-dash line), and 3) the star formation rate convolved with a distribution of time delays (dotted line, Totani et al., 1997). GRB 970508 (circle), GRB 971214 (cross) and GRB 980703 (triangle) are indicated, given their measured redshifts and the energy $\mathcal{E}_{tot}$ required to produce a burst at this redshift (given its total fluence, see text). Note that no single standard candle energy can accomadate the observed redshifts of these bursts, in any of the three models.

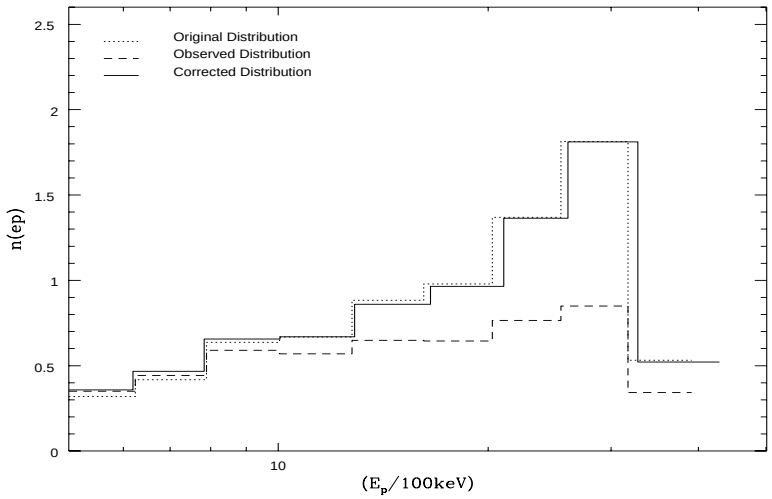

Fig. 6.— The original E_p distribution (solid line), the observed E_p distribution given the criterion $F_{obs} > F_{lim}$ (dashed line), and the corrected distribution using the method described in §2 of the text (dotted line). These distributions are obtained from the simulations described in the Appendix. Note that the procedure recovers the original distribution almost exactly. Any differences are primarily due to differences in the binnings of the distributions.